Proceedings of the International Conference on Industrial Engineering and Operations Management

Publisher: IEOM Society International, USA DOI: 10.46254/WC02.20250149
Published: October 14, 2025

Evaluation of Electroluminescence Performance of LEEC Based on Carbazole Derivative in D–A–Ph–D' Architecture

Sohrab Nasiri, Juozas Padgurskas and Raimundas Rukuiza
Department of Mechanical
Energy and Biotechnology Engineering
Vytautas Magnus University, Akademija, Lithuania
sohrab.nasiri2017@gmail.com

Abstract

This study reports the design and synthesis of a carbazole-based molecular donor–acceptor–phenyl–donor′ (D–A–Ph–D') architecture tailored for application in light-emitting electrochemical cells (LEECs). A thermally activated delayed fluorescence (TADF) emitter, derived from a carbazole scaffold was obtained by a coupling strategy. A reduced singlet–triplet energy gap (ΔE_{ST} = 0.07 eV), allowing efficient reverse intersystem crossing (RISC). The integration of this luminophore into LEEC devices resulted in a responsive electroluminescence (EL) behavior, in which the EL spectra exhibited green color, accompanied by an increase in external quantum efficiency (EQE) to 2.07%. Moreover, the incorporation of the ionic iridium complex Bis[2-(4-tert-butylphenyl)quinolinato-N,C]iridium(III) [4-(3,5-dimethyl-1H-pyrazol-1-yl)pyridine] hexafluorophosphate $[Ir(buoppy)_2(dmapzpy)]PF_6$ as a ionic host significantly improved the device performance, leading to a remarkable increase in luminosity. These results emphasize the synergistic role of TADF emitters and iridium-based hosts in improving the efficiency and adaptability of LEEC technology.

Keywords
LEECs; TADF; Carbazole; $[Ir(buoppy)_2(dmapzpy)]PF_6$; EQE

1. Introduction
Light-emitting electrochemical cells (LEECs) emerged in the mid-1990s as a simpler, and more cost-effective alternative to organic light-emitting diodes (OLEDs) with multiple layers. In their classic form, a single active film consisting of an emitting semiconductor (a conjugated polymer or an ionic transition metal complex) mixed with a low concentration of mobile ions from a salt, ionic liquid, or ionic gel is embedded between two electrodes (Pei et al., n.d.). When a voltage is applied, the ions drift; cations accumulate near the cathode and anions near the anode, forming electrical double layers (DLs) that dramatically lower the injection barriers and allow ohmic electron and hole injection even with air-stable electrodes (Lin et al., 2023). With sustained bias, the ions do more than just shield electrochemical doping occurs, creating n- and p-doped regions that propagate inward from the cathode and anode, respectively, until a dynamic p–n junction forms within the film; radiative recombination occurs in this junction region, the position of which can change with driving conditions and time (Lin et al., 2023). Depending on the material and waveform, LEECs can operate in an initial capacitive/double layers (DL) regime (fast turn-on dominated by interfacial charge) and a longer doping regime (transition-controlled emission), with color and efficiency determined by the emitting species and local doping levels (Katsumata et al., n.d.). The main attractions of LEECs are their simple architecture (often a single layer), compatibility with solution processing and printing on flexible substrates, tolerance to imperfect work function matching (thanks to self-regulating injection), low drive voltages, and the wide choice of emitters, which include conjugated polymers, ionic iridium or copper complexes, and advanced TADF luminophores (Meier et al., 2014),(Nasiri et al., 2024). These features make LEECs attractive for large-area, lightweight, and even stretchable illumination were manufacturability and cost trump ultimate performance (Wong and Zysman-Colman, 2017). The drawbacks are also well known; ion agitation can slow turn-on and lead to transient behavior; electrochemical reactions and ion-assisted

degradation pathways limit operating lifetime compared to the best on OLEDs; efficiency can suffer from non-radiative quenching in heavily doped zones or from transition drift, and careful control of electrolyte composition, encapsulation, and driving protocols (e.g., pulsed or alternating current) is required. Careful control of electrolyte composition, encapsulation and drive protocols (e.g., pulsed or AC operation) is required to mitigate aging, ion redistribution, and water/oxygen sensitivity (Hauenstein et al., 2020). Ongoing research is addressing these issues through more robust ion and salts, emitter designs with small singlet–triplet gaps TADF or stable iTMCs, engineering ion conductivities to achieve a balance between doping kinetics and stability, and device and drive technology that stabilizes the emission zone overall making LEECs more efficient, durable, and application-ready light sources (Maness et al., 1996).

Donor–acceptor–phenyl–donor′ (D–A–Ph–D') TADF dyes place an electron-acceptor core between two donors, with one donor coupled through a phenyl spacer that weakens conjugation and enforces a larger D–A dihedral angle. This topology localizes the highest occupied molecular orbitals (HOMO (s)) on the donor (s) and the lowest unoccupied molecular orbitals (LUMOs) on the acceptor while the phenyl spacer reduces HOMO–LUMO overlap, yielding a small ΔE_{ST} (typically <0.1 eV) yet preserving reasonable oscillator strength. Using unequal donors (D ≠ D′) enables color tuning and can promote symmetry-breaking charge-transfer in polar media, often increasing photoluminescence quantum yield (PLQY) and stabilizing emission. The phenyl bridge, and added steric bulk, helps suppress aggregation/excimer formation in films, improving color purity and limiting spectral red-tails. Well-optimized D–A–Ph–D' emitters show room-temperature RISC rates on the order of support efficient OLED/LEEC operation. In devices, hosts with high triplet energy and moderate polarity are preferred to stabilize the charge transfer (CT) state without over-red-shifting; tuning donor strength and spacer twist balances radiative rate against ΔE_{ST}. In this study the carbazole derivate was considered and photophysical and electroluminescence were investigated.

2. Experimental

The chemicals and solvents were purchased from Merck (analytical grade) and used without further purification. UV–vis absorbance spectra were recorded using an AvaSpec-ULS2048XL-EVO spectrometer controlled by AvaSoft 8. Steady-state photoluminescence (PL) spectra were recorded using a Hitachi F-4600 integrating sphere fluorescence spectrophotometer with, a xenon discharge lamp as excitation source; PL signals were measured at 400–800 nm. Low temperature phosphorescence spectra were measured using a cryostat under vacuum with liquid nitrogen cooling. Electroluminescence (EL) spectra were recorded using the AvaSpec-ULS2048XL-EVO (AvaSoft 8). Current–voltage–luminance (I–V–L) characteristics were measured using a Keithley 2400 SourceMeter (SMU) for electrical bias, an Ocean Optics spectrometer for emission, and a Mastech MS6612 optical meter for luminance.

Synthesis of dye

To synthesize the dye, the precursors were dissolved in toluene and heated under reflux. The mixture is gradually cooled and the organic layer is separated based on Ref (Rabiei et al., 2025). The crude product was purified by silica gel column chromatography using a mixture of THF and hexane. The synthesis pathway of the designed molecule is shown in Figure 1.

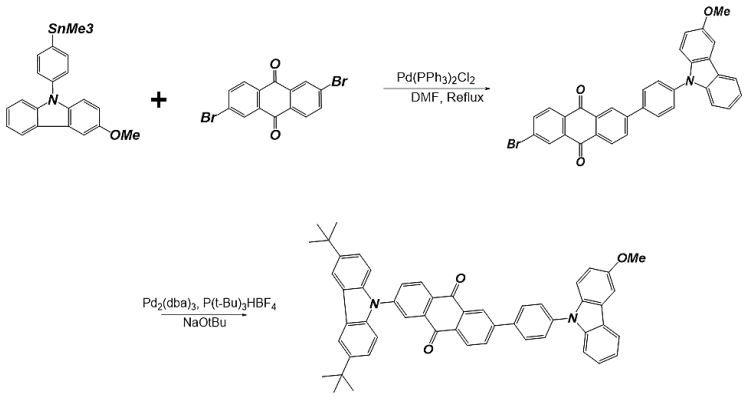

Figure 1. The designed and synthesized emitter

3. Results and Discussion

Photophysical properties

An absorption spectrum is a diagram that shows how strongly a material absorbs light depending on the wavelength or photon energy. Absorbance spectra are used to identify chromophores, quantify concentrations, determine oscillator strengths, track reaction kinetics, and select emitter/host elements in optoelectronic devices. Figure 2 shows a normalized absorption spectrum of the coated synthetic dye on the film, falling from about 266 nm to the visible region, with a long edge extending to about 500 nm. The strong UV band at 266 nm is consistent with π→π* transitions of the conjugated backbone (e.g., the carbazole moiety). A shoulder band at 410–500 nm indicates a weaker contribution from charge transfer (ICT/CT) or aggregated states superimposed on the main band (Yersin, 2018). The pronounced tail of the optical gap at 481 nm indicates edge states and/or intermolecular interactions aggregation, microstructural disorder that broaden the edge in the films, which was calculated to be 2.57 eV. Furthermore, the small absorption band at about 340 nm is also attributed to the n→π* transition (Zhang et al., 2010).

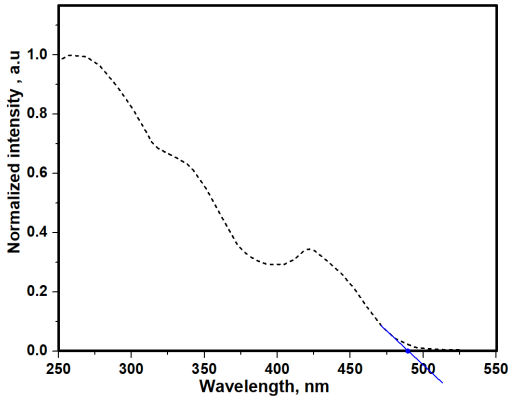

Figure 2. Absorption spectra of coated dye on the film

The normalized photoluminescence (PL) spectrum (Figure 3) shows a single, broad band peaking at 548 nm with a distinct red-skewed tail extending high wavelength. The absence of resolved vibronic structure and the large full width at half maximum (FWHM) indicate emission dominated by an intramolecular charge-transfer (ICT) state rather than a rigid, locally excited π→π* transition (Reichardt and Welton, 2010). The steep blue edge and extended red tail are consistent with microenvironmental heterogeneity and weak intermolecular interactions (e.g., excimer/exciplex contributions or aggregation) that populate lower-energy emissive sites, a behavior often observed for carbazole derivative donors paired with acceptors. Relative to the absorption onset, the position of the PL maximum implies a substantial Stokes shift, reflecting significant excited-state reorganization and matrix stabilization of the ICT state. In film matrices typically enhance interchain coupling, broadening the spectrum and strengthening the red tail. The spectral shape alone does not evidence TADF, but it is compatible with an ICT emitter that could support a small ΔE_{ST}; confirmation requires time-resolved PL showing a delayed component with the same spectral envelope as the prompt emission. For comprehensive reporting, quantify the absolute PLQY (integrating sphere), perform temperature-dependent PL (77 K to suppress aggregate channels), assess solvent-polarity and concentration dependences (film), and deconvolve the band (Gaussian/Lorentzian) to separate single-molecule and aggregate/exciplex contributions. Overall, the broad green emission is characteristic of carbazole derivative based ICT luminophores and is attractive for solution-processed devices, although mitigating aggregation will improve color purity and spectral stability.

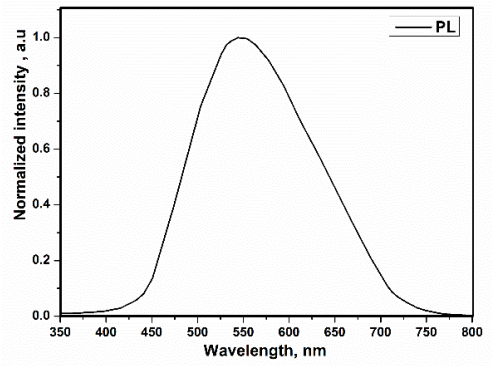

Figure 3. PL spectra of coated dye on the film

The plot in Figure 4, compares the steady-state fluorescence (black, PL) with the low-temperature phosphorescence (red, PH) of a carbazole-derived emitter. The PL trace shows a single broad band cantered in the green with a pronounced band consistent with emission from an ICT state in a heterogeneous matrix. The PH trace is red-shifted and broader, with a shoulder on the high-energy side and a long red tail band, features typical of triplet emission from a CT manifold and/or weak aggregate contributions stabilized at low temperature. On the blue edge, linear extrapolations mark the spectral onsets used to estimate the transition energies of the lowest singlet and triplet states. From the indicated values, E_S=2.84 eV and E_T=2.80 eV, giving a small singlet–triplet gap ΔE_{ST} = 0.07 eV. Such a narrow gap is favourable for thermally activated reverse intersystem crossing (RISC) and is consistent with TADF-capable ICT emitters, although confirmation requires time-resolved photoluminescence showing a delayed component with the same spectral envelope as the prompt PL and oxygen-quenching/temperature-dependence consistent with triplet harvesting (Zhang et al., 2012),(Goushi et al., 2012). Molecule TADF can use gentle room-temperature heat to turn normally "dark" triplet states back into light-emitting singlet states. So, it gets a quick flash (prompt fluorescence) plus a faint, later glow (delayed), letting devices use almost **all** excitons for higher efficiency without heavy metals. The substantial Stokes shift between the absorption onset (not shown here) and the PL maximum, together with the broadened, red-skewed profiles of both PL and PH, points to significant excited-state reorganization and aggregation effects in the solid. For device relevance, the small ΔE_{ST} suggests RISC activation energy (Tsai et al., 2019) and the potential for high exciton utilization, while the extended red tail flags the need to manage aggregation to preserve color purity and spectral stability.

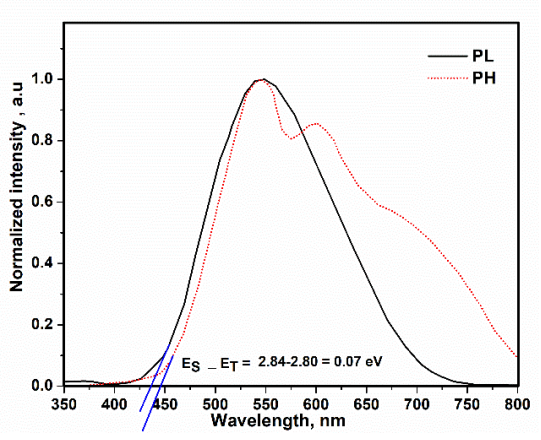

Figure 4. PL and PH spectra of coated dye on the film (at 77K)

Electroluminescence performance

Figure 5 shows a single-layer LEC; ITO (anode) / active layer (carbazole derivative-based dye + ionic iridium complex $[Ir(buoppy)_2(dmapzpy)]PF_6$) / LiF/Al (cathode). The diagram also shows the levels of the dye (HOMO = −5.72 eV, LUMO = −2.27 eV) and the work functions of the electrodes (ITO = −4.70 eV, LiF/Al = −2.90 eV). When a bias voltage is applied, the mobile ions from the iridium salt redistribute; PF_6 drifts to the anode ITO and the cations ($[Ir(buoppy)_2(dmapzpy)]^+$) to the cathode. This first builds up electrical double layers that collapse the injection

barriers, and then induces in-situ electrochemical doping of the neutral dye; p-doping near ITO (balanced by PF_6) and n-doping near Al (balanced by the iridium cation). The two doped regions grow inwards until a dynamic p–n junction is formed approximately in the middle of the film, where electrons and holes recombine radiatively. This self-regulating transition is the hallmark of LEECs and the reason why they work with a single active layer. Starting from the static planes, the nominal barriers are significant ITO→HOMO; Al→LUMO. In an OLED, these mismatches would be fatal, but in an LEEC they are neutralized by ion-driven band bending and doping, resulting in near-ohmic injection after turn-on. The thin LiF under Al further facilitates electron injection in the early (pre-doped) phase. The carbazole dye is the primary emitter and transport matrix, and the ionic Ir(III) complex provides mobile ions (ionic conductivity) and can act as a host/sensitizer, enabling energy transfer between host and guest förster resonance energy transfer (FRET)/dexter to the dye, while assisting in charge balancing. The result is low voltage operation and compatibility with solution processing. The design should exhibit fast turn-on after an initial ionic rearrangement, a stable emission zone near the center of the film, and improved EL when the Ir host supports energy transfer and injection. The typical LEEC caveats still apply: Ion movement can broaden spectra and shift color with drive; long-term stability depends on electrolyte formulation, encapsulation, and drive protocol (pulsed AC is often helpful). Reducing aggregation in the dye matrix and tuning the ion content improves color purity and lifetime.

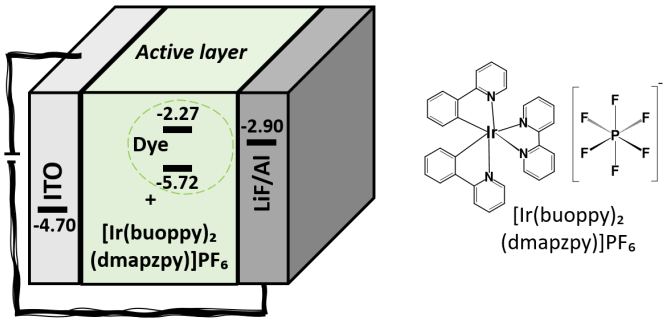

Figure 5. Scheme of LEEC device and chemical structure of $[Ir(buoppy)_2(dmapzpy)]PF_6$

Based on Figure 6, the device shows a single, broad electroluminescence band centered at 572 nm (greenish yellow). The lack of a vibronic substructure and the broad band indicate that the emission is dominated by an ICT rather than a rigid, locally excited transition typical of carbazole-based donor scaffolds in ionic matrices. Compared to the PL maximum reported for this dye, the EL peak is moved a little bit, which could be due to stronger polarization of the medium and field-assisted stabilization of the CT state in the LEEC transition, slight local heating under bias, and/or partial formation of weak aggregate environments in the p–n emission zone (Shin et al., 2007). The overall symmetry of the band and the relatively confined red tail indicate that excimer/exciplex contributions are not dominant under the present driving conditions. Since the spectrum is normalized, its shape suggests good color stability within the measured current range, but the LEECs may exhibit time-dependent drift as the doped regions move; tracking the spectrum as a function of time/current (constant current aging) is recommended. For reporting, extract the CIE 1931 coordinates, the current peak would shift the color near the greenish yellow region, specify the FWHM, and overlay PL against EL to highlight the EL shift. If TADF is expected from this ICT emitter, confirm by time-resolved EL/PL delayed component consistent with the prompt spectrum and temperature/oxygen dependence. Overall, the single EL band with moderate width is consistent with CT-dominated emission from a stable recombination zone in the LEEC, suitable for devices in solution process, while further suppression of aggregation would improve color purity and spectral stability.

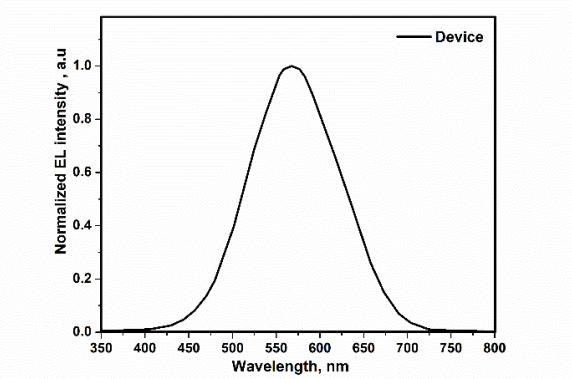

Figure 6. EL spectrum of fabricated LEEC device

The Figure 7 plot shows the efficiency of the device as a function of luminance. The efficiency starts at very low brightness, then increases as the injection stabilizes, a p–n region gradually forms in the LEEC, and the effective series resistance decreases, it then gradually decreases the value at several thousand cdm^{-2} as the current increases. The initial increase is due to the completion of ion rearrangement and charge balance enhancement, while the decrease at high luminance is caused by joule heating, triplet–triplet annihilation (TTA) and exciton–polaron quenching, field-induced dissociation, and ion redistribution/transition drift; any EL at high current further lowers lmW^{-1} by decreasing photopic weighting. For reporting, give the peak value and corresponding luminance along with efficiencies; to improve the curve, lower the driving voltage optimize electrodes/LiF and carrier mobility, mitigate quenching at high currents appropriate host dilution and reduced aggregation, and stabilize the emission zone by pulsed/AC driving.

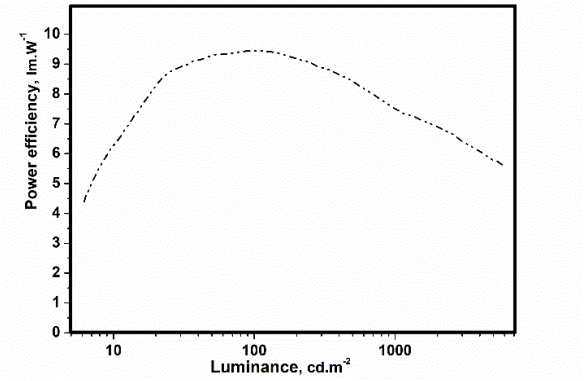

Figure 7. Power efficiency versus luminance of fabricated LEEC device

This plot in Figure 8 shows external quantum efficiency (**EQE) vs luminance**. The maximum EQE at **2.03 %** rises as injection stabilizes and a p–n region forms, then **rolls off** with increasing current. The initial rise reflects completion of ionic rearrangement and a lower effective drive voltage; the high-luminance roll-off is attributed to Joule heating, TTA, exciton–polaron quenching, field-induced dissociation, and ion redistribution/junction drift. To mitigate roll-off, employ pulsed/AC driving, dilute the emitter in a suitable host, reduce aggregation, and optimize emissive-layer thickness and injection (e.g., LiF/electrode configuration).

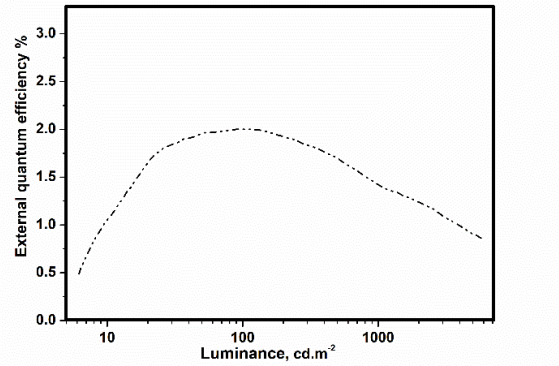

Figure 8. External quantum efficiency versus luminance of fabricated LEEC device

This plot in Figure 8 shows EQE vs luminance. The maximum EQE at 2.03 **%** rises as injection stabilizes and a p–n region forms, then rolls off with increasing current. The initial rise reflects completion of ionic rearrangement and a lower effective drive voltage; the high-luminance roll-off is attributed to Joule heating, TTA, exciton–polaron quenching, field-induced dissociation, and ion redistribution/junction drift. To mitigate roll-off, employ pulsed/AC driving, dilute the emitter in a suitable host, reduce aggregation, and optimize emissive-layer thickness and injection e.g., LiF/electrode configuration.

4. Conclusions

We have designed and synthesized a carbazole-based TADF emitter and demonstrated its functionality in single-layer electrochemical light sources (LEECs) using the ionic iridium complex $[Ir(buoppy)_2(dmapzpy)]PF_6$ in the active layer. Photophysical analysis shows broad photoluminescence with charge transfer character. Combined PL–PH measurements at low temperature 77K reveal low singlet–triplet splitting 0.07 eV, consistent with efficient RISC and triplet collection. In the devices, ion-assisted formation of p/n-doped regions and a dynamic transition enables balanced injection and electroluminescence. The LEECs exhibit a peak EQE of 2.03 % with a corresponding increase in power efficiency at intermediate luminance, followed by the expected drop at high brightness due to joule heating and exciton–polaron annihilation losses. The iridium salt acts as both ion source and host/sensitizer, which improves charge balance and luminosity, while the CT emitter provides the small ΔE_{ST} needed for TADF-assisted emission. Overall, these results demonstrate a practical, solution-processed route to LEECs that utilizes the synergy between a TADF dye and an iridium host. Further optimization of the host-to-dye ratio, ion content, film morphology, and driving protocol e.g., pulsed/AC operation should suppress aggregation, stabilize the emission zone, and mitigate the efficiency drop.

Acknowledgment

This project has received funding from the Research Council of Lithuania (LMTLT), agreement No. S-PD-24-174.

References

Goushi, K., Yoshida, K., Sato, K., Adachi, C., Organic light-emitting diodes employing efficient reverse intersystem crossing for triplet-to-singlet state conversion. Nature Photonics 6, 253–258, 2012. https://doi.org/10.1038/nphoton.2012.31

Hauenstein, C., Gottardi, S., Bobbert, P.A., Coehoorn, R., Van Eersel, H., Effects of exciton deconfinement on the transient photoluminescence from thermally activated delayed fluorescence host–guest systems. Journal of Applied Physics 128, 075501, 2020. https://doi.org/10.1063/5.0019073

Lin, Y.D., Lu, C.W., Su, H.C., Long-Wavelength Light-Emitting Electrochemical Cells: Materials and Device Engineering. Chemistry – A European Journal 29, e202202985, 2023. https://doi.org/10.1002/CHEM.202202985

Maness, K.M., Terrill, R.H., Meyer, T.J., Murray, R.W., Wightman, R.M., Solid-State Diode-like Chemiluminescence Based on Serial, Immobilized Concentration Gradients in Mixed-Valent Poly[Ru(vbpy)3](PF6)2 Films. Journal of the American Chemical Society 118, 10609–10616, 1996. https://doi.org/10.1021/JA953185W

Meier, S.B., Tordera, D., Pertegás, A., Roldán-Carmona, C., Ortí, E., Bolink, H.J.,Light-emitting electrochemical cells: recent progress and future prospects. Materials Today 17, 217–223, 2014. https://doi.org/10.1016/J.MATTOD.2014.04.029

Nasiri, S., Rabiei, M., Shaki, H., Hosseinnezhad, M., Kalyani, K., Palevicius, A., Vilkauskas, A., Janusas, G., Nutalapati, V., Kment, S., Michel Nunzi, J., What is TADF (thermally activated delayed fluorescence) compared to the mechanisms of FL (fluorescence), PH (phosphorescence), and TTA (triplet–triplet annihilation) based on a novel naphthalimide sulfonylphenyl derivative as a host? Journal of Photochemistry and Photobiology A: Chemistry 447, 115289, 2024. https://doi.org/10.1016/J.JPHOTOCHEM.2023.115289

Pei, Q., Yu, G., Zhang, C., Yang, Y., Heeger, A.J., Polymer Light-Emitting Electrochemical Cells 10, 2024.

Rabiei, M., Ghahary, R., Hosseinnezhad, M., Palevicius, A., Vilkauskas, A., Janusas, G., Nasiri, S., Nunzi, J.M., Padgurskas, J., Rukuiza, R., Light-emitting electrochemical cells based on mechanochromic, thermally activated delayed fluorescence fish-shaped structures consisting of carbazole derivatives as emitters in the active layer. Organic Electronics 141, 107214, 2025. https://doi.org/10.1016/J.ORGEL.2025.107214

Reichardt, C., Welton, T., Solvents and Solvent Effects in Organic Chemistry: Fourth Edition. Solvents and Solvent Effects in Organic Chemistry: Fourth Edition, 2010. https://doi.org/10.1002/9783527632220

Shin, J.H., Matyba, P., Robinson, N.D., Edman, L., 2007. The influence of electrodes on the performance of light-emitting electrochemical cells. Electrochimica Acta 52, 6456–6462, 2007. https://doi.org/10.1016/J.ELECTACTA.2007.04.068

Tsai, K.W., Hung, M.K., Mao, Y.H., Chen, S.A., Solution-Processed Thermally Activated Delayed Fluorescent OLED with High EQE as 31% Using High Triplet Energy Crosslinkable Hole Transport Materials. Advanced Functional Materials 29, 1901025, 2019. https://doi.org/10.1002/ADFM.201901025

Wong, M.Y., Zysman-Colman, E., Purely Organic Thermally Activated Delayed Fluorescence Materials for Organic Light-Emitting Diodes. Advanced Materials 29, 1605444, 2017. https://doi.org/10.1002/ADMA.201605444;REQUESTEDJOURNAL:JOURNAL:15214095;WGROUP:STRING:PUBLICATION

Yersin, H., Highly Efficient OLEDs, Highly Efficient OLEDs: Materials Based on Thermally Activated Delayed Fluorescence. Wiley-VCH Verlag GmbH & Co. KGaA, Weinheim, Germany, 2018. https://doi.org/10.1002/9783527691722

Zhang, H., Wan, X., Xue, X., Li, Y., Yu, A., Chen, Y., Selective Tuning of the HOMO–LUMO Gap of Carbazole-Based Donor–Acceptor–Donor Compounds toward Different Emission Colors. European Journal of Organic Chemistry 2010, 1681–1687, 2010. https://doi.org/10.1002/EJOC.200901167

Zhang, Q., Li, J., Shizu, K., Huang, S., Hirata, S., Miyazaki, H., Adachi, C., Design of efficient thermally activated delayed fluorescence materials for pure blue organic light emitting diodes. Journal of the American Chemical Society 134, 14706–14709, 2012. https://doi.org/10.1021/JA306538W/SUPPL_FILE/JA306538W_SI_001.PD